doi.org/10.36721/PJPS.2024.37.3.REG.499-509.1

Aloe vera leaf mucilage and lemon oil as potential penetration-enhancing agents to increase lornoxicam transdermal administration using nano vesicular gel

Gopinath Subramaniyan[1], Shaik Rubina[2]*, Bachu Venkata Ramana[3], A Meriton Stanley[4] and Devasena Srinivasan[5]

[1]Department of Pharmaceutics, Faculty of Pharmacy, Sri Ramachandra Institute of Higher Education and Research (DU), Tamil Nadu, India
[2]Research scholar, Department of Pharmacy, Sri Ramachandra Institute of Higher Education and Research (DU), Tamil Nadu, India
[3]Department of Pharmaceutics, Dr. K. V. Subba Reddy Institute of Pharmacy, Andhra Pradesh, India
[4]Department of Community Medicine, SRMC & RI, Sri Ramachandra Institute of Higher Education and Research (DU), Chennai, India
[5]Department of General Medicine, SRMC & RI, Sri Ramachandra Institute of Higher Education and Research (DU), Chennai, India

Abstract: The goal of the existing work was to create matrix transdermal patches with lornoxicam (LXM) gel using lemon oil (LO) and *Aloe vera* leaves mucilage (AVLM) as penetration enhancers to boost LXM transport crossways the skin and test its *in vivo* analgesic effects. Nine formulas were produced for this purpose using Design Expert® 11 in line with CCD design. The response factors, on the other hand, were Q_{1d} (Y_1), Q_{2d} (Y_2) and Q_{3d}, or LXM permeation at days 1, 2 and 3. The AVLM concentration (X1) and lemon oil (X2) were selected as independent variables. The optimized patch's skin sensitivity response and analgesic activity were tested on rats. The results exhibited that a matrix system with prolonged (zero-order) LXM release of 24.15% (@24h), 49.00% (@48h), and 69.45% (optimized for the needed analgesic asset by using AVLM and LO as penetration enhancers. It was resolute that the formulation known as LTDP-8, which contains 3mL of AVLM and LO as permeability enhancers, is the best one. In light of its ability to administer LXM across the skin sustainably while producing a tolerable analgesic effect. The study concludes that the artificial transdermal LXM delivery system is a suitable substitution for the oral route.

Keywords: Analgesic, design, lornoxicam, patch, permeation.

INTRODUCTION

Non-steroidal anti-inflammatory medications (NSAIDs) are frequently employed to make transdermal patches (TDP) that deliver analgesic possessions (Aziziaram *et al*., 2021). NSAID-TDP are more practical and secure than its oral form. Different NSAID tablets were given to the rheumatoid arthritis patient. NSAID-TDP can prevent adverse possessions such as stomach bleeding, increased acidity and ulcers (Krathumkhet *et al*., 2021). The site of a bruise, sprain, or strain may be treated with an NSAID analgesic patch (Shi *et al*., 2013). When these TDPs are employed on the skin, the drug penetrates the skin, subcutaneous adipose tissue and muscle at levels adequate to have local therapeutic possessions without raising plasma drug concentrations (Ahad *et al.,* 2016; Khan *et al*., 2020; Shravani *et al*., 2021; Jyothika *et al.,* 2022). As a result, NSAIDs have the benefit of improving local medication distribution to the afflicted tissues while having a lower incidence of systemic adverse possessions. Patients with rheumatoid arthritis are encouraged to use NSAIDs for an extended period; however, the main disadvantages of NSAID medications are their systemic toxicity and GIT irritation (Sehajpal *et al.,*2000).

A strong NSAID of the oxicam class is lornoxicam (LXM). It is frequently employed for analgesic and inflammatory and uncomfortable chronic diseases (Belal *et al*., 2020; He *et al*., 2020). Oral use of LXM causes a variety of gastrointestinal, renal and haematological side effects, just as do other NSAIDs (Shah *et al.,* 2019). Aside from them, its brief half-life necessitates regular administration (every 3-4h). Additionally, it is not advised to use parenteral administration for long-term disorders.

To prevent LXMs from permeating the skin, the epidermis serves as an ideal barrier. Transdermal LXM delivery has been improved with the introduction of various chemical enhancers. To prevent LXMs from permeating the skin, the epidermis serves as an ideal barrier (Swetha *et al*., 2010). Transdermal LXM delivery has been improved with the introduction of various chemical enhancers. These substances reversibly modify the skin's barrier function, enabling molecules with low penetration to pass through the stratum corneum and eventually reach the bloodstream (Ahad *et al.,* 2010; Quan *et al.,* 2021). Numerous studies have demonstrated that when combined, penetration enhancers can generate a synergistic action that promotes skin permeation more excellently than when employed alone (Ananda *et al.,* 2021). Co-solvents are frequently employed in TDP as

**Corresponding author:* e-mail: rubinanizamm@gmail.com

carriers and penetration boosters. These substances improve the LXM's solubility while also changing the skin's structure to increase penetration. Consequently, both LXM discharge and penetration are impacted (Yadav and Urade, 2019).

Several fatty acids, particularly lemon oil, have been utilized to enhance percutaneous LXM absorption (OA). In many TDPs, the usage of LO with *Aloe vera* leaf mucilage (AVLM) proves to be a particularly active combination (Kovacik *et al.,* 2020).

Studies using AVLM and LO as potential penetration-enhancing agents are available in the literature. But no studies reported using these combinations and optimization with a central composite design. To increase the transdermal permeability of LXM, the current work uses AVLM and LO co-solvent as penetration enhancers. To do this, the matrix-type TDP with LXM that can regulate the discharge at a steady pace for 7 days.

MATERIALS AND METHODS

Materials

Waksman Selman Pharmaceuticals Ltd., Anantapur, donated lornoxicam, triethanolamine, lemon oil (OA), carbopol 934P and HPLC-grade methanol (Fischer Scientific, India). *Aloe vera* leaves contain mucilage and adhesive tape USP (Leukoplast) (which works as a backing layer and adhesive layer) was brought from the medical store Anantapur.

Animals

Wistar Albino Rats (male, weighing 150-200g) were attained from the animal house of K.V. Subba Reddy Institute of Pharmacy, Kurnool, India after taking institutional animal ethical committee (54/A of U022100867/ 2022 and 1953/PO/Re/S/17/CPCSEA) were utilised for tests on analgesic asset and skin irritation. Good laboratory practices were followed for the attention and use of rats. The animals were kept in typical lab settings with unrestricted access to food and water (Hindustan *et al.,* 2012; Ramadan *et al.,* 2018).

Solubility studies of LXM

Separate conical flasks containing water and 10mL of phosphate buffer saline (PBS) with pHs of 5.8, 6.8 and 7.4 received more LXM powder. The flasks were continuously shaken in an orbital shaker bath for 72h (Remi RS-12R). A sample was extracted and run through a 0.45µm Millipore filter. The dilution was measured spectrophotometrically at 376 nm (thrice and an average was taken) (Kharwade *et al.,* 2012; Dasgupta *et al.,* 2014).

Experimental design

The tests were planned using Design-Expert version 11 and a CCD (Stat-ease, USA). LXM discharge at Q_{1d}, Q_{2d} and Q_{3d} were regarded as dependent response factors, whilst AVLM (X_1) and LO (X_2) were picked as factors (table 1). The polynomial equation was created for each response and the optimum formulation was chosen based on the outcomes (Ahad *et al*., 2021; Babu *et al.,* 2022; Yadiki *et al.,* 2022).

Formulation of LXM gel

Carbopol 934 P (C-934P) was soaked in water overnight to make the gel. Then, triethanolamine was employed to dissolve a specific amount of LXM. 10mL of water, AVFM, LO and methylparaben were dissolved in the LXM mixture while being continuously stirred. Until a homogenous gel was produced, the solvent mixture was combined with the C-934P and stirred for an additional 20 min (Madan *et al.,* 2016; Shah *et al*., 2019; Din *et al.,* 2022; Latif *et al.,* 2022).

Physicochemical description of LXM gel

The LXM gels' colour, homogeneity, viscosity, pH and LXM concentration were appraised. A pH meter that was calibrated was employed to find the pH (Mettler MP-220, Switzerland). The viscosity of gel at 25°C was done with a Brookfield viscometer (Wellon PHMTR001), with the spindle speed set to 20 rpm. There were three duplicates of each test run (He *et al*., 2020; Tawfeek *et al.,* 2020).

Making of LTDP

A magnetic stirrer was employed to dissolve the quantities of HPMC K-15, C-934P and AVLM (table 1) in a 1:1 (methanol: dichloromethane) solvent, creating 9 batches of Lornoxicam transdermal patches (LTDPs) (100 rpm at 25^{o}C). LXM and methylparaben were added and combined after this. To create an LXM layer, the mixture was placed onto Petri dishes that had been greased with glycerine and kept in a 40°C oven for one hour. The LTDPs were then wrapped in a fabric backing film (EVA). The LTDPs adhesive side was then covered by a liner (PVP) (Shah *et al*., 2019; Hashmat *et al.,* 2020). Then kept in a desiccator until usage (fig. 1).

Weight and thickness of fabricated LTDP

Weighed three LTDPs were randomly selected from each formulation and each was weighed independently. Next, the standard deviation and weight average were appraised.

The thickness of the LTDPs were measured at each of their four corners and in the centre using a micrometre screw gauge. SD with an average thickness was used to represent the findings.

Content uniformity of LTDPs

Get a sample ready. Using 100mL of PBS pH 7.4, LXM was removed from the reservoir slot. The flask was shaken with a motorised shaker for four hours (Vibe X). After the solution had been filtered, the HPLC method was used to determine the LXM content.

HPLC analysis. With a few minor modifications, the Kavitha and Rajendra (Kavitha and Rajendra, 2011) HPLC method was used to measure LXM. The HPLC with C-18 column (250X4.6 mm, 5µm particle size), a Shimadzu 20AD pump and a Shimadzu SPD-20A UV detector). The samples were sensed at 376 nm (Shimadzu's Lab Solutions software). In the mobile phase, methanol and aqueous phosphate buffer (6:4 v/v) and 1 M caustic soda was used to raise the pH to 7. The sample was injected and the flow rate was 1mL per min. LOD and LOQ were assessed to be 0.1 and 0.5µg/mL, consequently.

A standard calibration curve for LXM was established in the concentration of 0-20µg/mL. To appraise linearity, LXM determination was done during the mobile phase. Good linearity between the LXM levels and the peak area of LXM was discovered, with great connexions (r^2=0.999). Using the generated standard curve, LXM content in LTDPs was estimated (Yadav and Urade, 2019; Hashmat *et al*., 2020).

In vitro permeation study

A Franz diffusion cell (FDC) with a receptor cubicle was used to conduct *in vitro* skin permeation studies (22.5mL). The donor and receptor booths of the FDC were implanted with the abdominal skin of Wistar albino rats. The paraffin film and LTDPs were employed on the skin.

The receptor partition of the FDC was filled with phosphate buffer, pH 7.4. The temperature was held constant at 32±0.5°C while the fluid in the receptor section was constantly and incessantly spun with magnetic beads at 50 rpm. A magnetic stirrer supported the entire contraption. At various times, samples were taken out and the LXM concentration was measured spectrophotometrically.

An identical volume of phosphate buffer pH 7.4 was poured into the receptor phase at the time of each sample removal. The cumulative % of LXM permeability per square centimetre of LTDPs was contrived with time (Baviskar *et al.,* 2013; El-Ridy *et al.,* 2018; Hashmat *et al*., 2020).

A variety of kinetic models, including the zero-order, first-order, Higuchi, Korsmeyer Peppas and Bidas models, were used to compute the discharge kinetics. The coefficient of correlation (r^2) and rate constants was calculated using the Excel Add-In Program PK Solver and the values of r^2 were compared to decide which model best fit the data.

Skin irritation study

The skin irritancy trials used the methods that Draize *et al.,* described. Three groups of six rats each were produced from the animals. Group III was given 0.8% formalin aqueous solution as the reference irritant, while Group II was treated with optimized LTDPs. Group-I served as the control group. The rats had their hair cut off 24 h before the test. After applying the LTDPs to the rat's skin, the site was protected and circled with an elastic adhesive bandage. It was possible to investigate the cutaneous reactions using the Draize method (Alepee *et al*., 2010; Modi *et al*., 2022).

In vivo analgesic activity

The analgesic action of LRX was performed by the hot-plate analgesic technique. There were three different animal groups, each with a total of six. Group II served as the reference group and got an oral dose of 4mg/kg LRX whereas Group III received the enhanced LTDPs as treatment. Group-I was the control group (4 cm^2). After 0, 30, 60, 120 and 180 min, the test LTDPs were applied to the rear of each rat's paw in the treatment group. Reaction times were then measured. To control the latency period, each rat was placed on a hot plate (Mage Engineers, India) that was kept at a temperature of 55±1^{o}C. Jumping, raising the leg and licking the back foot are a few examples of reactions to pain stimuli. We continuously monitored the rats for any apparent behavioural abnormalities, illness and mortality (Maurya *et al*., 2019; Abdallah *et al*., 2021; Begum *et al*., 2021).

STATISTICAL ANALYSIS

One-way ANOVA was availed with Design export software (Ver. 11) to analyse the variances between control and treated groups *in vivo* investigations. P>0.05 was availed as the cut-off point for statistical significance. The statistical analyses were done with SPSS (V-20).

RESULTS

Solubility of LXM

The solubility of medicine is crucial for achieving the right bioavailability. Low water solubility is the main challenge that novel therapeutic compound research faces. Most drugs have poor aqueous solubility with mildly basic/acidic. One of the medications with poor aqueous solubility is LXM. Studies on the LXM's solubility in water, PEG-600, PEG-400, propylene glycol, tween-80, tween-20 and phosphate buffers were conducted (pH 5.8, 6.8 and 7.4).

Characterization of gels

Each gel had enough aesthetic qualities like homogeneity, a smooth texture, consistent colour and no phase separation (table 2). The pH range for gel compositions LTDP-1 through LTDP-9 is 6.32±0.04 to 6.89±0.12.

Characterization of LTDPs

A 30 cm^2 surface area LTDPs was created and its weight, thickness and LXM homogeneity were all appraised. The average weight and thickness of LTDPs were indomitable

to be 6.16±0.19g to 6.95±0.62g and 1.58±0.01mm to 1.71±0.08mm, respectively.

The LTDPs were appraised for weight, thickness and LXM homogeneity. Their surface area was 30 cm^2. LTDPs were estimated to have an average weight and thickness of 6.16±0.19µg to 6.95±0.62µg and 1.58±0.01 mm to 1.71 0.08 mm, consequently.

In vitro permeation observations

The rate and quantity of LXM permeation from a TDP can be accurately assessed by an *in vitro* LXM permeation experiment. The permeation of LXM from the LTDPs mostly controls how LXM is delivered in the matrix LTDPs (table 3 and fig. 2) and the release followed zero-order release kinetics (table 4).

Formulation optimization

A CCD was selected for the LTDPs optimization. For each of the two parameters, there were three levels of evaluation available and all nine possible combinations were tested in experiments. The independent factors were AVLM (X_1) and LO (X_2) and the responses were Q_{1d} (Y_1), Q_{2d} (Y_2) and Q_{3d} (X_2). A polynomial statistical model that was interactive was used to appraise the responses.

$$Y=b_0+b_1X_1+b_2X_2+b_{12}X_1X_2+b_{11}X_1^2+b_2^2X_2^2$$

Y denotes the dependent variable in this equation, b_0 denotes the arithmetic mean of the nine runs and bi denotes the estimated coefficient for the factor Xi. Effects (X_1) and (X_2) demonstrate what happens when one element is changed from a low to a high value at a time. The interaction phrases are used to describe how a reaction changes when two elements are changed at once (X_1X_2). The polynomial terms (X_{21}) and (X_{22}) are combined to look for nonlinearity. Data analysis was done using Design-Expert 11, a tool (Stat ease, Minneapolis, MN).

The findings unambiguously reveal that the LXM permeation at 24h 4 h and 72h was highly reliant on the independent factors used. The best-fitting model was found to be the quadratic one. To create simplified models, $P>0.05$ insignificant terms were removed. The terms with $P<0.05$, however, were thought to be statistically significant and were kept in the simplified models. The following equations were constructed for the condensed quadratic models Q_{1d} (Y_1), Q_{2d} (Y_2) and Q_{3d} (Y_3):

$$Q_{1d}=+27.60-0.1386A-0.3034B+0.7850AB+0.3406A^2-1.46B^2$$

$$Q_{2d}=+48.70-0.4953A+0.5350B+0.1750AB-0.6938A^2-0.2438B^2$$

$$Q_{3d}=+65.80-1.24A+2.26B+0.1725AB-2.46A^2-0.3987B^2$$

Skin irritation observations

It is critical to evaluate how well these formulations interact with the skin because TDP is meant to be applied to the skin. The pressure-sensitive adhesives used to attach to the PTDP may result in skin reactions. To control the skin's sensitivity to the TDP being used, a skin irritation study is necessary. The study's findings on skin irritation were acceptable (fig. 4 and table 6).

In vivo analgesic activity

The hot-plate test Hot-plate experiments with Wister albino rats were conducted to gauge the analgesic potency of the prepared LTDPs.

Their tolerance or resistance to the feeling of heat up until they licked their paws or jumped was an indication of the analgesic action of the LTDPs. The results of this study expressed, as indicated in table 8, that the newly developed LTDPs had a considerable analgesic outcome on thermal pain stimuli.

DISCUSSION

The solubility results exhibited that water had the lowest solubility (5.29±0.02mg/mL), while phosphate buffer pH 7.4 had the maximum solubility (11.08±0.07mg/mL). These outcomes were similar to the conclusions of Fatima *et al* (Fatima *et al*., 2021) where the solubility was more in phosphate buffer 7.4 and was found to be 10.34± 0.23mg/mL.

The pH levels were discovered to be suitable for TDP production, being closer to neutral (pH 7). The gels' LXM concentrations were found to be within the intended range of 90-110% (96.95±2.48 to 99.54±0.68%) and their viscosities ranged from 3158±23.69 to 3807±19.85 cps.

The LTDPs showed a small variance in the weight and thickness of the formulations. The content homogeneity ranged from 96.95±2.48 to 99.58±3.25%, indicating strong LXM uniformity across all LTDPs. The results exhibited that the weight and thickness of the formulations varied only slightly. Content homogeneity between 96.95±2.48 to 99.58±3.25% demonstrated good LXM consistency across all the LTDPs.

The formulation LTDP-8 had the highest 72h discharge (69.45±1.95%), followed by formulation LTDP-1 (65.80±1.33%), while formulations LTDP-2 and LTDP-6 exhibited a 59% discharge.

To investigate the release kinetics, data from *in vitro* LXM discharge investigations were plotted in a range of kinetic models, including zero-order, first-order, Higuchi, Korsmeyer-Peppas and Bidas. All LTDP with R^2 values ranging between 0.9565 and 0.9885, fit best with the zero-order model (table 4). The discharge exponent "n" indicates the type of diffusion implied by the LTDPs. "n"-values between 0.5 and 1 were found in the current experiment, indicating non-Fickian transports.

Table 1: Constituents of LTDP

Formulation	Lornoxicam (g)	HPMC K-15	C-934P (g)	A:AVLM	B:LO	Methyl paraben (g)	Triethanolamine (g)	Distilled water (mL)
LTDP-1	0.8	0.5	0.5	1	1	0.2	2	100
LTDP-2	0.8	0.5	0.5	5	1	0.2	2	100
LTDP-3	0.8	0.5	0.5	1	5	0.2	2	100
LTDP-4	0.8	0.5	0.5	5	5	0.2	2	100
LTDP-5	0.8	0.5	0.5	0.17157	3	0.2	2	100
LTDP-6	0.8	0.5	0.5	5.82843	3	0.2	2	100
LTDP-7	0.8	0.5	0.5	3	0.17157	0.2	2	100
LTDP-8	0.8	0.5	0.5	3	5.82843	0.2	2	100
LTDP-9	0.8	0.5	0.5	3	3	0.2	2	100

Table 2: Physicochemical characteristics of LXM gel

Formulation	pH	Viscosity (cps)	Weight (g)	Thickness (mm)	Drug content (%)
LTDP-1	6.81±0.25	3200±21.25	6.52±0.35	1.59±0.06	99.58±3.25
LTDP-2	6.89±0.12	3158±23.69	6.58±0.65	1.65±0.08	98.15±2.32
LTDP-3	6.54±0.52	3625±32.52	6.23±0.82	1.63±0.07	97.25±1.25
LTDP-4	6.58±0.02	3728±36.38	6.28±0.15	1.61±0.02	97.18±1.65
LTDP-5	6.32±0.04	3581±48.25	6.45±0.44	1.69±0.03	99.08±2.16
LTDP-6	6.45±0.09	3419±14.15	6.95±0.62	1.58±0.01	96.95±2.48
LTDP-7	6.66±0.12	3349±16.39	6.34±0.48	1.64±0.06	98.46±0.17
LTDP-8	6.72±0.05	3807±19.85	6.16±0.19	1.67±0.05	99.54±0.68
LTDP-9	6.81±1.66	3465±20.85	6.34±0.97	1.71±0.08	97.82±1.32

Values in mean ±S.D; n=3

Table 3: Responses from the LTDP

Formulation	Response 1 Q_{1d} (%)	Response 2 Q_{2d} (%)	Response 3 Q_{3d} (%)
LTDP-1	27.70	47.70	62.03
LTDP-2	26.00	46.50	59.02
LTDP-3	25.56	48.50	65.30
LTDP-4	27.00	48.00	62.98
LTDP-5	28.50	48.20	63.12
LTDP-6	27.90	46.60	59.85
LTDP-7	25.06	47.60	61.77
LTDP-8	24.15	49.00	69.45
LTDP-9	27.60	48.70	65.80

Table 4: The correlation (r^2) values for LXM discharge from LTDPs

Patch	Correlation (r)						
	Zero order	First order	Higuchi	Hixson Crowell's	Korsmeyer Peppas	n	Release mechanism
LTDP-1	0.9838	0.9196	0.9867	0.9745	0.6876	0.6999	NF
LTDP-2	0.9795	0.9418	0.9564	0.9638	0.6670	0.7287	NF
LTDP-3	0.9885	0.9227	0.9514	0.9888	0.6619	0.7413	NF
LTDP-4	0.9695	0.8768	0.9701	0.9655	0.6344	0.7580	NF
LTDP-5	0.9703	0.9182	0.9349	0.9512	0.6333	0.7641	NF
LTDP-6	0.9565	0.9685	0.9565	0.9513	0.6117	0.7923	NF
LTDP-7	0.9692	0.8728	0.9815	0.9065	0.6042	0.8090	NF
LTDP-8	0.9845	0.7987	0.9507	0.8917	0.5969	0.8172	NF
LTDP-9	0.9882	0.9568	0.9419	0.8808	0.5424	0.8849	NF

NF: Non-fickian

Table 5: Statistics for the quadratic model's model summary

Responses	Std. Dev.	%CV	Adequate precision	R^2	Adjusted R^2	Predicted R^2	F-value	P-value	Commence
Y_1	0.1815	0.6821	28.4789	0.9943	0.9849	NA*	105.58	0.0014	significant
Y_2	0.1946	0.4066	15.1774	0.9813	0.9502	NA*	31.50	0.0085	significant
Y_3	1.2467	1.9708	8.9228	0.9433	0.8490	NA*	9.9986	0.0434	significant

*Case(s) with leverage of 1.0: Pred R^2 and PRESS statistic not defined.

Table 6: Skin irritation study of optimized LTDPs

Rat no	Control		Formalin		LTDPs	
	Erythema	Oedema	Erythema	Oedema	Erythema	Oedema
1	0	0	3	2	1	0
2	0	0	2	1	1	1
3	0	0	1	1	1	0
4	0	0	2	2	0	0
5	0	0	3	1	1	1
6	0	0	1	2	1	0
Average	0	0	2	1.5	0.834**	0.334**

**p<0.01, significant
a:Erythema scale: 0- no erythema; 1- very slight erythema;
2-Well-defined erythema; 3-moderate to severe erythema.
b:Oedema scale: 0- no oedema; 1-very slight oedema;
2-slight oedema; 3-moderate oedema.

Table 7: The analgesic outcome of optimized LTDP

Group	Treatment		Reaction time (sec) 0 min	30 min	60 min	120 min	180 min
I	Control		38.22±0.29	41.25±0.13	42.87±0.86	39.51±0.91	41.47±0.64
II	Standard	Paw licking	40.12±0.25	46.91±0.62**	53.81±0.51**	58.85±0.54**	63.66±0.12**
III	Test		39.36±0.85	47.82±0.14**	52.15±0.14**	56.05±0.17**	61.54±0.18**
I	Control		77.85±0.81	78.28±1.52	78.71±0.77	77.84±1.24	78.51±0.59
II	Standard	Jump Response	79.22±0.95	85.74±0.85**	91.19±0.52**	98.25±0.82**	102.02±0.15**
III	Test		77.15±0.41	87.48±0.95**	92.33±0.22**	97.45±0.21**	103.52±0.91**

**P<0.01, significantly different from control (Tukey's multiple comparison post–hoc test); mean ± SD; n = 6

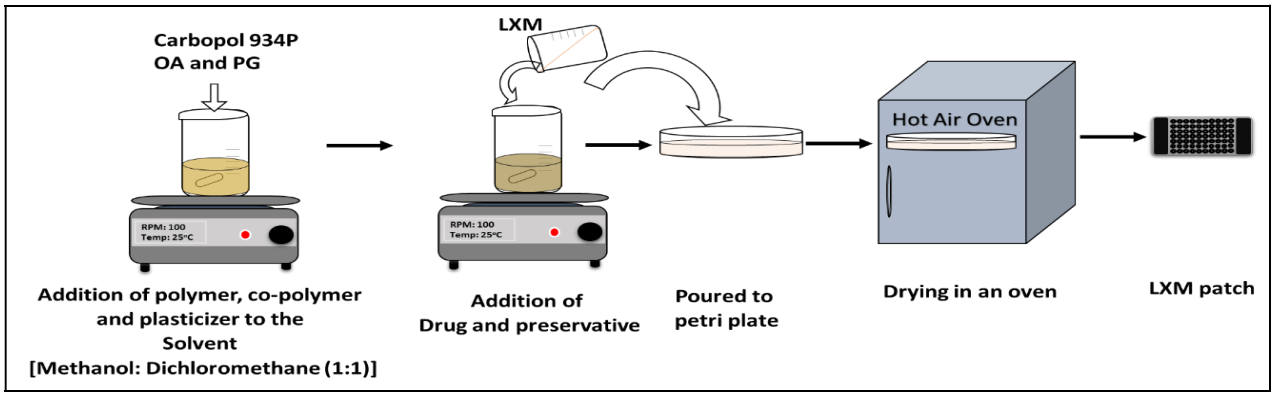

Fig. 1: Pictorial representation of making of LTDP

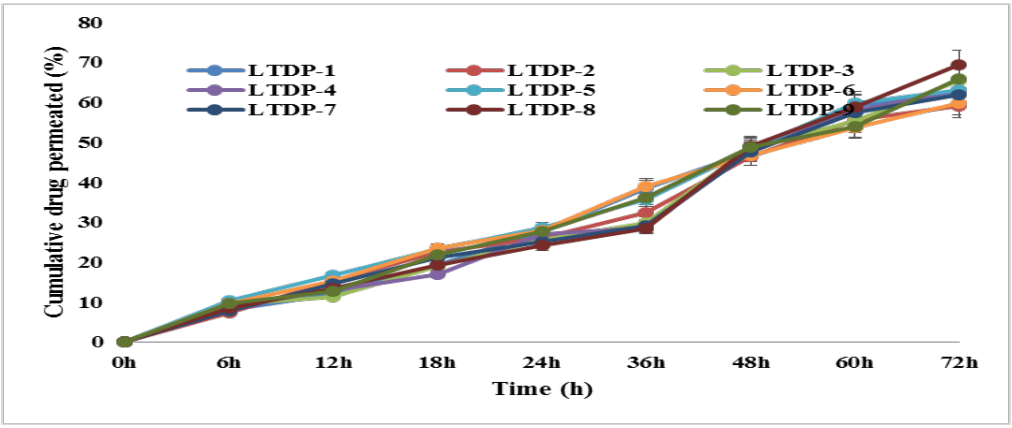

Fig. 2: *In vitro* drug release of LXM

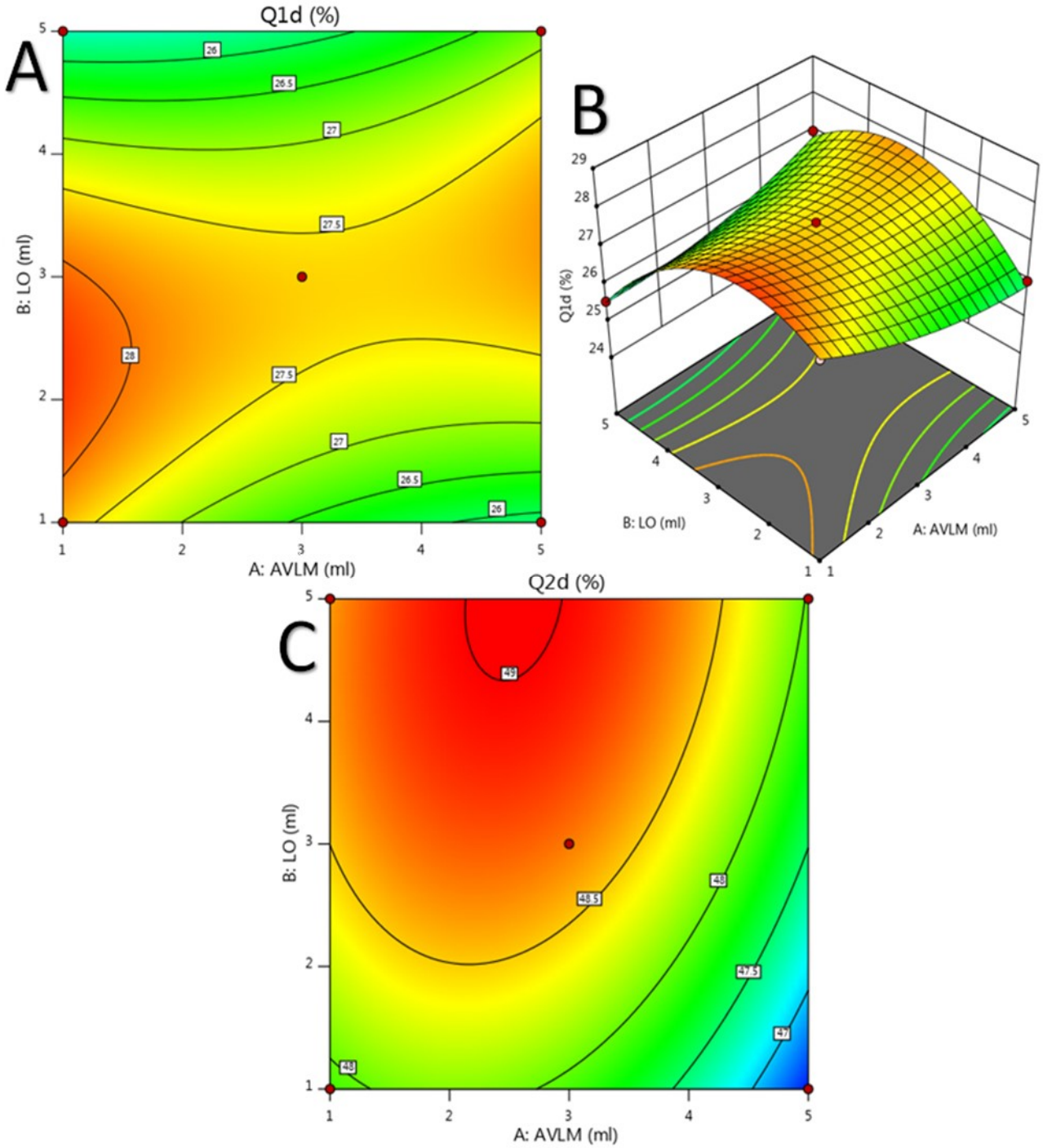

According to table 5's summary statistics for condensed quadratic models, the modified r^2 for responses Y_1, Y_2 and Y_3 is largely consistent with the anticipated r^2 values. The optimum formulation of the LXM matrix LTDPs with Q_{1d} (24.15%), Q_{2d} (24.15%) and Q_{3d} (69.45%) was appraised to be LTDP-8, which contained 0.5g of C-934P, 3mL of each of AVLM and LO and 0.5g of C-934P. In Fig. 5, contour and 3D response surface plots appear that the use of the mid-value of AVLM and LO resulted in appreciable permeation.

Draize *et al.* define hazardous chemicals as those that produce scores of 2 or less or no skin irritation. Therefore, it was permitted to utilise the LTDPs. The skin irritation study confirms that the prepared gel is non skin irritant.

Thriveni *et al.* revealed similar outcomes (Thriveni *et al*., 2020). According to statistics, there was significant variance between the test and control group's reaction times ($P<0.01$). However, it was uncovered that there was no significant variance between the test group's reaction time and the standard group's ($P>0.05$).

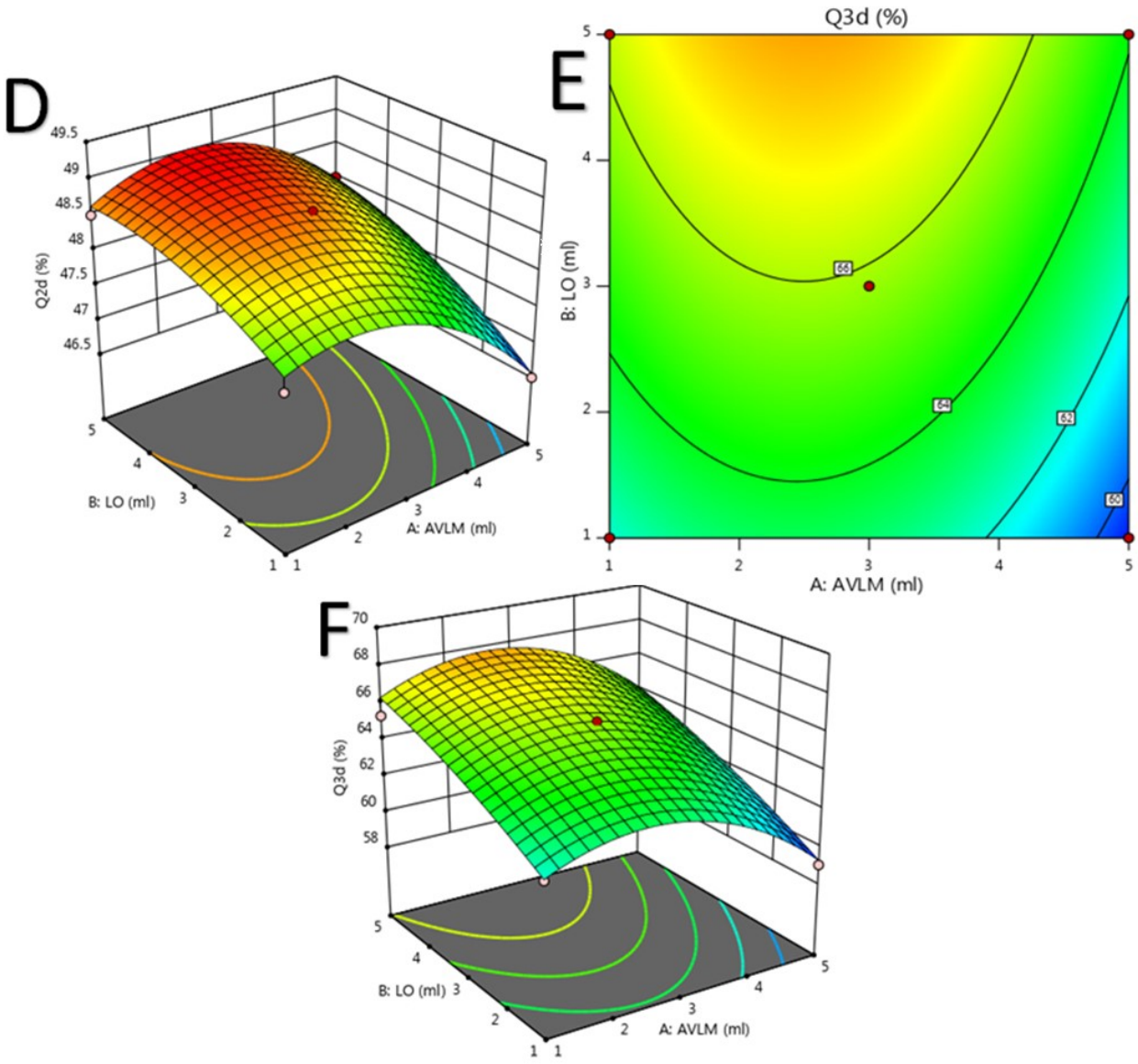

Fig. 3: Contour plots (A) Q_{1d} (C) Q_{2d} (E) Q_{3d} and responses surface curves (B) Q_{1d} (D) Q_{2d} (F) Q_{3d} for optimization of LTDP

In vivo analgesic activity confirms the ananlgesic activity of the prepared gel. Thriveni *et al.* revealed similar outcomes (Thriveni *et al*., 2020). According to statistics, there was significant variance between the test and control group's reaction times ($P<0.01$). However, it was uncovered that there was no significant variance between the test group's reaction time and the standard group's ($P>0.05$).

According to Vosooghi and Amini, 2014, COX enzyme inhibition is the primary mechanism through which NSAIDs exert their outcomes (Vosooghi & Amini, 2014). There are two isomeric variants of COX: COX_1 and COX_2. LXM was uncovered to have strong COX_1 and COX_2 inhibitory properties as well as pronounced analgesic assets (Hashmat *et al*., 2020; Tayal, 2012) and LXM was ten times more active than LXM at preventing carrageenan-induced paw swelling in ancillary urged polyarthritic rats.

CONCLUSION

These transdermal patches can be used as an alternative to oral administration of lornoxicam (LXM) to deliver an active therapeutic dose with better patient compliance, fewer gastrointestinal side effects and reduced dosing frequency. Based on its LTDP can be used as an alternative to oral administration of LXM to deliver an active therapeutic dose with better patient compliance, fewer gastrointestinal side effects and reduced dosing

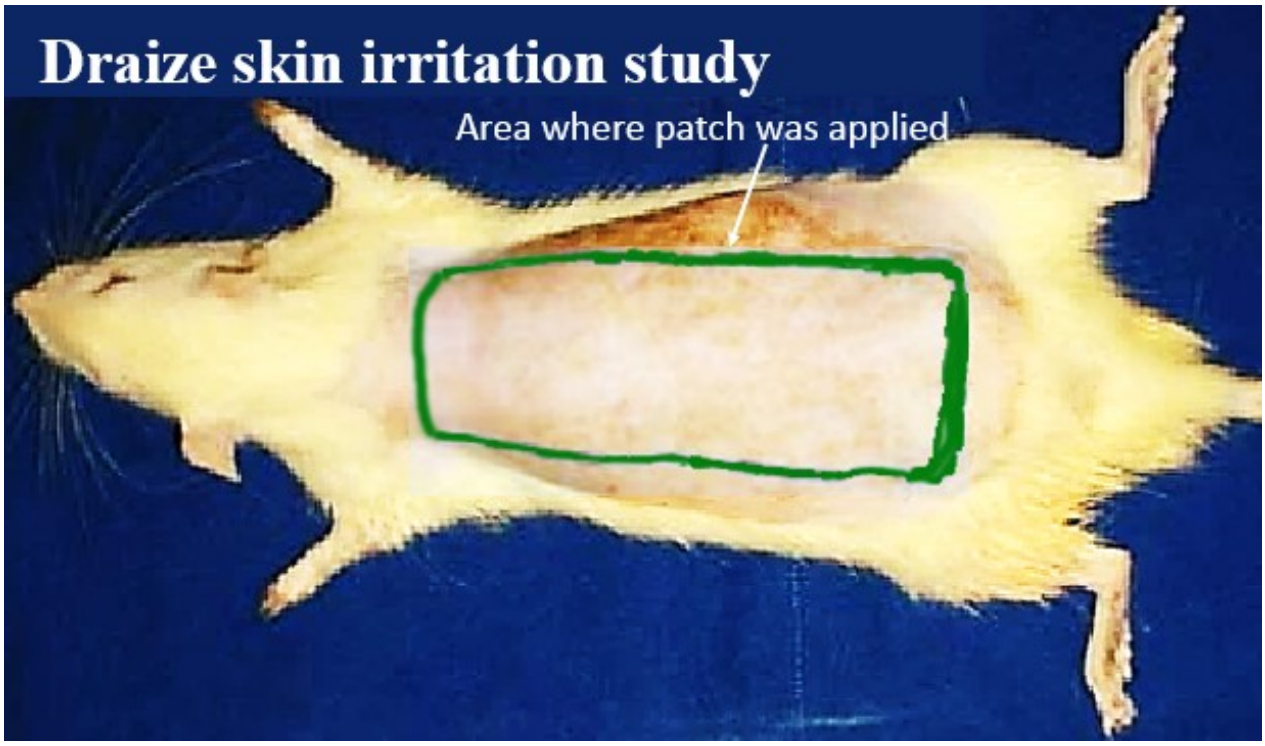

Fig. 4: Draize skin irritation studies on the back of the albino rats

frequency. It was found that using AVLM and LO as penetration enhancers increased the flow of LXM through the skin without causing any discomfort. The built-in matrix patches and their study generated the impression that herbal-oriented permeation enhancers (AVLM and LO) could be employed to speed up the penetration of LXM through the skin from LXM gel patches. It was found that using AVLM and LO as penetration enhancers increased the flow of LXM through the skin without causing any discomfort. The built-in matrix patches and their study generated the impression that herbal-oriented permeation enhancers (AVLM and LO) could be employed to speed up the penetration of LXM through the skin.

REFERENCES

Abdallah MH, Lila ASA, Unissa R, Elsewedy HS, Elghamry HA and Soliman MS (2021). Preparation, characterization and evaluation of anti-inflammatory and anti-nociceptive effects of brucine-loaded nanoemulgel. *Colloids Surf. B,* **205**(3): 111868.

Ahad HA, Chinthaginjala H, Rahamtulla S, Pallavi BP, Shashanka C and Prathyusha J (2021). A comprehensive report on solid dispersions by factorial design. *Asian J. Res. Chem.,* **14**(4): 297-301.

Ahad HA, Ishaq BM, Shaik M and Bandagisa F (2016). Designing and characterizing of tramadol hydrochloride transdermal patches prepared with Ficus carica fruit mucilage and povidone. *Pak. Jour. Pharma. Sci.,* **29**(3): 945-951.

Ahad HA, Kiranmaye N, Yasmeen R, Ruksana H and Muneer S (2010). Designing and evaluation of glimepiride ficus glomerata fruit mucilage matrix transdermal patches. *Asian J. Chem.,* **22**(4): 2935.

Alepee N, Tornier C, Robert C, Amsellem C, Roux MH, Doucet O and de Fraissinette AdB (2010). A catch-up validation study on the reconstructed human epidermis (SkinEthic™ RHE) for full replacement of the Draize skin irritation test. *Toxicol. In vitro,* **24**(1): 257-266.

Ananda PWR, Elim D, Zaman HS, Muslimin W, Tunggeng MGR and Permana AD (2021). Combination of transdermal patches and solid microneedles for improved transdermal delivery of primaquine. *Int. J. Pharm.*, **609**(4): 121204.

Aziziaram Z, Bilal I, Zhong Y, Mahmod AK and Roshandel MR (2021). Protective effects of curcumin against naproxen-induced mitochondrial dysfunction in rat kidney tissue. *Cell. Mol. Biomed. Reports,* **1**(1): 23-32.

Babu GN, Menaka M and Ahad HA (2022). Neem fruit mucilage-aided mucoadhesive microspheres of acyclovir using 32 factorial design with design-expert software. *Appl. Biol. Res*., **24**(1): 17-27.

Baviskar DT, Parik VB and Jain DJ (2013). Development of Matrix-type transdermal delivery of lornoxicam: *In vitro* evaluation and pharmacodynamic and pharmacokinetic studies in albino rats. *PDA J. Pharm. Sci. Tech.,* **67**(1): 9-22.

Begum MY, Alqahtani A, Ghazwani M, Ramakrishna M, Hani U, Atiya A and Rahamathulla M (2021). Preparation of Carbopol 934 based ketorolac tromethamine buccal mucoadhesive film: *In vitro*, *ex vivo* and *in vivo* assessments. *Int. J. Polymer Sci.,* Article ID 4786488, 1-11.

Belal F, Omar MA, Derayea SM, Zayed S, Hammad MA, Saleh SF and Al Bratty M (2020). Direct injection microemulsion hplc method for simultaneous determination of morphine, tramadol and lornoxicam in biological fluids using monolithic column. *Curr. Pharm. Analysis,* **16**(8): 1148-1156.

Dasgupta S, K Ghosh S, Ray S, Singh Kaurav S and Mazumder B (2014). *In vitro* and *in vivo* studies on lornoxicam loaded nanoemulsion gels for topical application. *Curr. Drug Del.,* **11**(1): 132-138.

Dinh L, Lee S, Abuzar SM, Park H and Hwang SJ (2022). Formulation, preparation, characterization and evaluation of dicarboxylic ionic liquid donepezil transdermal patches. *Pharmaceutics*, **14**(1): 205-211.

El-Ridy MS, Yehia SA, Mohsen AM, El-Awdan SA and Darwish AB (2018). Formulation of niosomal gel for enhanced transdermal lornoxicam delivery: *In-vitro* and *in-vivo* evaluation. *Curr. Drug Del.,* **15**(1): 122-133.

Fatima K, Bukhari NI, Latif S, Afzal H, Hussain A, Shamim R and Abbas N (2021). Amelioration of physicochemical, pharmaceutical and pharmacokinetic properties of lornoxicam by cocrystallization with a novel coformer. *Drug Dev. Ind. Pharm.,* **47**(3): 498-508.

Hashmat D, Shoaib MH, Ali FR and Siddiqui F (2020). Lornoxicam controlled release transdermal gel patch: Design, characterization and optimization using co-solvents as penetration enhancers. *Plos One,* **15**(2): e0228908.

He Y, Majid K, Maqbool M, Hussain T, Yousaf AM, Khan IU and Younus A (2020). Formulation and characterization of lornoxicam-loaded cellulosic-microsponge gel for possible applications in arthritis. *Saudi Pharm. J.,* **28**(8): 994-1003.

Hindustan AA, Babu UA, Nagesh K, Kiran DS and Madhavi KB (2012). Fabrication of glimepiride Datura stramonium leaves mucilage and poly vinyl pyrrolidone sustained release matrix tablets: *In vitro* evaluation. *Kathmandu Uni. J. Sci. Eng. Tech.,* **8**(1): 63-72.

Jyothika LSK, Ahad HA, Haranath C, Kousar S and Sadiya SH (2022). Types of transdermal drug delivery systems: A literature report of the past decade. *RJPDFT,* **14**(2): 157-162.

Kavitha K and Rajendra MM (2011). Design and evaluation of transdermal films of lornoxicam. *Int. J. Pharma. Bio. Sci.,* **2**(2): 54-62.

Khan D, Qindeel M, Ahmed N, Khan AU, Khan S nad Rehman AU (2020). Development of novel pH-sensitive nanoparticle-based transdermal patch for management of rheumatoid arthritis. *Nanomedicine,* **15**(06): 603-624.

Kharwade M, Achyuta G, Subrahmanyam C and Sathesh Babu P (2012). Solubility behavior of lornoxicam in binary solvents of pharmaceutical interest. *J. Solu. Chem.,* **41**(8): 1364-1374.

Kováčik A, Kopečná M and Vávrová K (2020). Permeation enhancers in transdermal drug delivery: Benefits and limitations. *Exp. Opi. Drug Del.,* **17**(2): 145-155.

Krathumkhet N, Imae T and Paradee N (2021). Electrically controlled transdermal ibuprofen delivery consisting of pectin-bacterial cellulose/polypyrrole hydrogel composites. *Cellulose,* **28**(18): 11451-11463.

Latif MS, Al-Harbi FF, Nawaz A, Rashid SA, Farid A, Mohaini MA, Alhashem YN (2022). Formulation and evaluation of hydrophilic polymer based methotrexate patches: *In vitro* and *in vivo* characterization. *Polymers*, **14**(7): 1310.

Madan JR, Ghuge NP and Dua K (2016). Formulation and evaluation of proniosomes containing lornoxicam. *Drug Del. Trans. Res.,* **6**(5): 511-518.

Maurya A, Rangappa S, Bae J, Dhawan T, Ajjarapu SS and Murthy SN (2019). Evaluation of soluble fentanyl microneedles for loco-regional anti-nociceptive activity. *Int. J. Pharm.,* **564**(6): 485-491.

Modi D, Nirmal J, Warsi MH, Bhatia M, Hasan N, Kesharwani P and Jain GK (2022). Formulation and development of tacrolimus-gellan gum nanoformulation for treatment of dry eye disease. *Colloids Surf. B,* **211**(2): 112255.

Quan P, Jiao B, Shang R, Liu C and Fang L (2021). Alternative therapy of rheumatoid arthritis with a novel transdermal patch containing siegesbeckiae herba extract. *J. Ethnopharmacol.*, **265**(1): 113294.

Ramadan E, Borg T, Abdelghani G and Saleh N (2018). Design and *in vivo* pharmacokinetic study of a newly developed lamivudine transdermal patch. *Fut. J. Pharm. Sci.,* **4**(2): 166-174.

Sehajpal S, Prasad DN and Singh RK (2018). Prodrugs of non-steroidal anti-inflammatory drugs (NSAIDs): A long march towards synthesis of safer NSAIDs. *Mini Rev. Med. Chem.,* **18**(14): 1199-1219.

Shah H, Nair AB, Shah J, Bharadia P and Al-Dhubiab BE (2019). Proniosomal gel for transdermal delivery of lornoxicam: Optimization using factorial design and *in vivo* evaluation in rats. *DARU J. Pharm. Sci.,* **27**(1): 59-70.

Shi Y, Wei Z, Zhao H, Liu T, Dong A and Zhang J (2013). Electrospinning of ibuprofen-loaded composite nanofibers for improving the performances of transdermal patches. *J. Nanosci. Nanotech.,* **13**(6): 3855-3863.

Shravani Y, Ahad HA, Haranath C, gari Poojitha B, Rahamathulla S and Rupasree A (2021). Past decade work done on cubosomes using factorial design: A fast

track information for researchers. *Int. J. Life Sci. Pharma. Res.,* **11**(1): P124-135.

Swetha T, Ahad HA, Reddy KK, Sekhar A, Sivaji S and Kumar B (2010). Formulation and *in-vitro* permeation studies of Ketoprofen-Ficus reticulata fruit mucilage transdermal patches. *Der Pharmacia Lettre,* **2**(6): 190-199.

Tawfeek HM, Abdellatif AA, Abdel-Aleem JA, Hassan YA and Fathalla D (2020). Transfersomal gel nanocarriers for enhancement the permeation of lornoxicam. *J. Drug. Del. Sci. Tech.,* **56**(1): 101540.

Tayal S (2012). The role of lornoxicam in pain and inflammation: A review. *Cur. Res. Pharm. Sci.*, **2**(1): 1-4.

Thriveni R, Rukhsar I, Ramesh DV, Patil S, Byatnal A and Nair D (2020). Development and clinical evaluation of transmucosal mucoadhesive patch of lornoxicam for the odontogenic pain management: A preliminary study. *J. Nat. Sci., Bio. Med.,* **11**(1): 12-16.

Vosooghi M and Amini M (2014). The discovery and development of cyclooxygenase-2 inhibitors as potential anticancer therapies. *Exp. Opi. Drug Discov.,* **9**(3): 255-267.

Wallace JL (2000). How do NSAIDs cause ulcer disease? *Best. Pract. Res. Clin. Gastroenterol.,* **14**(1): 147-159.

Yadav AV and Urade MN (2019). Formulation and evaluation of chitosan-based transdermal patches of lornoxicam for prolonged drug release and to study the effect of the permeation enhancer. *Indian J. Pharm. Educ. Res,* **53**(1): 88-96.

Yadiki MN, Suggala VS, Puchalapalli DSR and Ahad HA (2022). Temperature and exposure time impact on the extraction of opuntia ficus-indica and opuntia dillenii cladodes on % yield as a response: Screening using design expert software. *GJMPBU,* **17**(17): 1-5.